Fractional Order Extremum Seeking Control; Performance and Stability Analysis

Hadi Malek, *Senior Member, IEEE,* YangQuan Chen, *Senior Member, IEEE*

***Abstract*—In this paper a novel extremum seeking control algorithm called fractional order extremum seeking control is analyzed and benchmarked against the traditional integer order one. Utilizing fractional order operators in extremum seeking scheme improves the convergence speed, robustness and performance of this method without adding complexity to the algorithm. Using averaging model, the detailed analysis of fractional order extremum seeking control is presented. Simulation and experimental results support the mathematical analysis and demonstrate that proposed scheme outperforms the traditional extremum seeking algorithm.**

***Index Terms*—Extremum seeking control, fractional order operators, nonlinear optimization.**

I. Introduction

EXtremum seeking control (ESC) is an online adaptive algorithm which attempts to determine the extremum (max or min) value of an unknown nonlinear performance function in real-time, thereby reduces the downtime by eliminating the need for offline data analysis. This extremum seeking method was successfully applied to a wide range of electromechanical engineering applications including maximum power point tracking in renewable energy systems [1], [2], [3], [4], [5], [6], control of ABS brakes [7], [8], [9], combustion engine timing control [10], [11], mobile robots path planing [12], [13], [14], [15] and so on. A descriptive survey on extremum seeking control and its applications can be found in [16] and [17].

Due to the wide range of engineering applications, there exist a growing interest among researchers and scientists to improve the performance and reliability of this algorithm by providing better fine tuning and calibration methods. Nesic in [18] has presented a tuning guidelines which will ensure larger domain of attraction and faster convergence speed for extremum seeking algorithm. In [18], author has claimed the global peak will be achieved in the presence of local extremum(s) if ESC parameters are tuned properly. In [3] and [14], researchers have improved this algorithm by adding a dynamic compensation within the feedback loop to increase the convergence speed. Tan and his colleagues have analyzed various periodic perturbation signals to improve convergence speed of the algorithm [19]. In other works, additional loops and/or complex mathematical blocks have been proposed to be added to the ESC structure in order to reduce the convergence speed and raise the performance of the system [3], [20], [21], [22], [14], [23], [24], [25], [26], [27], [28].

In this paper, to improve the transient response of ESC, a novel extremum-seeking scheme for the optimization of nonlinear plants utilizing fractional order calculus is proposed. A detailed stability analysis of this Fractional Order Extremum Seeking Control (FO-ESC) scheme is provided to guarantee the convergence of the system to an adjustable neighborhood of the optimum. Furthermore, as will be demonstrated, special features of fractional order operators, such as *locality* and *generalized stability criteria* improve the most important criteria for extremum seeking schemes; convergence speed and robustness. In addition, unlike other proposed ESC schemes in the literature, neither additional feed-back/feed-forward loops nor complex mathematical calculations (e.g. matrix calculation) is required for the proposed FO-ESC in order to improve the performance and convergence speed of the system. This feature simplifies the implementation of the FO-ESC and reduces the calculation time and implementation cost. In order to compare FO-ESC and IO-ESC, an averaged linearized model of FO-ESC is derived and analyzed against the equivalent averaged linearized model for IO-ESC. Comparing these two models illustrates the aforementioned advantages of fractional order operators utilization in the ESC.

In order to compare FO-ESC and IO-ESC, an averaged linearized model of FO-ESC is derived and analyzed against the equivalent average linearized model for IO-ESC. Comparing these two models illustrates the advantages of applying fractional order operators into the ESC algorithm.

The rest of the paper is organized as follows: Section II introduces the fractional order calculus. Section III presents an overview of extremum seeking algorithm. In Sections IV, the proposed FO-ESC is introduced and analyzed. Simulation and experimental results are presented in section V. Concluding remarks are presented in section VI.

II. Fractional Order Derivatives and Integral Definitions

The idea of fractional calculus has been known since the development of the regular calculus, with the first reference probably being associated with letter between Leibniz and L'Hospital in 1695 [29].

Grunwald-Letnikov (GL) and Riemann-Liouville (RL) are two of the most popular definitions which are widely used in various literature [30]. The GL which is the discrete definition

Hadi Malek is with the Utah State University, Utah, USA, email: h.m.malek@ieee.org

YangQuan Chen is with the University of California, Merced, CA, USA, email:yqchen@ieee.org

Manuscript received Mar. 20, 2015; revised Sept. 20, 2015.

is defined as

$$ {}_aD_t^{\alpha} f(t) = \lim_{h\to 0} h^{-\alpha} \sum_{j=0}^{[\frac{t-a}{h}]} (-1)^j \binom{\alpha}{j} f(t-jh), \qquad (1) $$

where [.] means the integer part of the number. The RL which is the continuous definition is defined as

$$ {}_aD_t^{\alpha} f(t) = \frac{1}{\Gamma(n-\alpha)} \frac{d^n}{dt^n} \int_a^t \frac{f(\tau)}{(t-\tau)^{\alpha-n+1}} d\tau, \qquad (2) $$

for $(n-1 < \alpha < n)$ and $\Gamma(.)$ is the *Gamma* function. When $a = 0$ sometime authors use D^{α} notation which is equal to ${}_0D_t^{\alpha}$.

In some special cases, Eq. (1) and Eq. (2) are not equivalent. More details regarding these two definitions and their differences have been discussed in [30]. Since all the analysis in this paper is in continuous domain, RL definition of fractional order differintegral is considered in this work. Some others important properties and applications of the fractional derivatives and integrals can be found in [31], [32], [33], [29], [34].

Since introduction of fractional calculus to engineering world, the modeling of physical phenomena using fractional order operators and fractional order controllers have been widely investigated among researchers and scientist in this field. All previous researches on the application of fractional order operators in the engineering field imply the superiority of the fractional order operators compared to the classical integer order ones from the view point of robustness and performance. [35], [36], [29], [37], [32], [30].

III. Extremum Seeking Algorithm

In recent years, various types of ESC structures have been introduced and investigated in the literature and among different algorithms, sinusoidal perturbed ESC structure has drown the most interest among researchers [17]. The general form of a single input-single output periodic perturbed extremum seeking scheme is shown in Fig. 1. As shown in this figure, this type of ESC employs a slow periodic perturbation, $\sin(\omega t)$, and add it to the estimated signal $\hat{\theta}$. Because of the slow dynamics of the perturbation signal, the plant appears as a static map $(y = f(\theta))$ to ESC and its dynamics does not interfere with the extremum seeking scheme [38]. If the estimated signal, $\hat{\theta}$, is on either side of the extremum point, θ^*, the perturbation, $a\sin(\omega t)$, creates a periodic response of y which is either in phase or out of phase with $a\sin(\omega t)$. The high-pass filter eliminates the "DC component" of y. Thus perturbation signal, $a\sin(\omega t)$, and output signals are two approximately sinusoidal waveform which are in phase if $\hat{\theta} < \theta^*$ or out of phase if $\hat{\theta} > \theta^*$ [38].

Figure 2 presents the ESC operation as described above. In this figure, the output of ESC algorithm has been depicted when the operating point is larger, equal or smaller than extremum point.

Since product of two in phase signals gives a signal with a positive mean and this product results a negative mean for two out of phase signal, this feature can be used to find the operating point using a gradient detector [39].

The mathematical model for ESC scheme (Fig. 1) can be written as

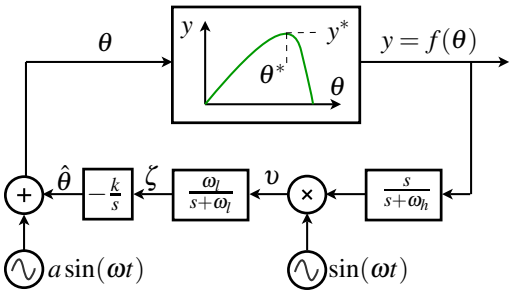

Fig. 1. Block Diagram of Periodic Perturbed Extremum Seeking Algorithm

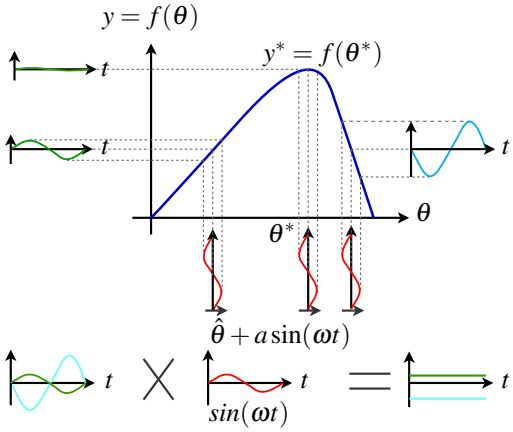

Fig. 2. Operation of Extremum Seeking Algorithm [39]

$$ \begin{cases} y = f(\hat{\theta} + a\sin(\omega t)) \\ \dot{\hat{\theta}} = -k\zeta \\ \zeta = \upsilon * \mathscr{L}^{-1}\{\frac{\omega_l}{s+\omega_l}\} \\ \upsilon = \left(y * \mathscr{L}^{-1}\{\frac{s}{s+\omega_h}\}\right)\sin(\omega t) \end{cases}, \qquad (3) $$

where '$*$' is the convolution operator and $\mathscr{L}^{-1}$ is the inverse Laplace transform.

To obtain the optimal performance of ESC loop, perturbation frequency, ω, amplitude, a, gradient update law gain, k, and filter cut-off frequencies, ω_h and ω_l must be tuned and calibrated adequately. Following general rules have been listed in literature as ESC design rules [23], [40]. To ensure that the plant dynamics will not be captured by ESC loop, the perturbation frequency must be selected such that it is slower than the slowest plant dynamics. Therefore plans appears as a static system to ESC. The cut-off frequencies of high-pass and low-pass filters must be designed in coordination with the perturbation frequency ω; $\omega_h < \omega$ and $\omega_l < \omega$. However, these filters should have sufficient bandwidth (higher cut-off frequencies) to be able to respond quickly to the control input perturbations. Although larger values for amplitude of perturbation signal, a, or gradient gain, k, results in faster convergence rates of ESC, but higher values of k and a increase the oscillation amplitude of the estimated signal and sensitivity of the system against external or internal disturbances.

A. Simplified Extremum Seeking Control Algorithm

Since low-pass filter and integrator are in series, in some literature, low-pass filter block is eliminated in the ESC structure [41], [17]. Moreover, some researchers claim that filters have no direct impact on the convergence speed of the algorithm and their role is to reduce the oscillation amplitude of the estimated signal [17]. For these reasons and to simplify analysis, without lose of generality, low-pass filter will be eliminated in this work ($\zeta = \upsilon$) and (3) becomes

$$\begin{cases} y = f(\hat{\theta} + a\sin(\omega t)) \\ \dot{\hat{\theta}} = -k\upsilon \\ \upsilon = \left(y * \mathscr{L}^{-1}\{\frac{s}{s+\omega_h}\}\right)\sin(\omega t) \end{cases}. \tag{4}$$

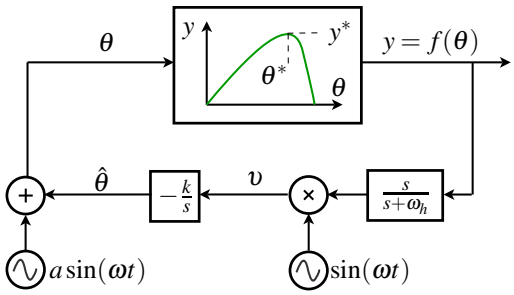

Fig. 3. Block Diagram of Reduced Order Extremum Seeking Algorithm

The stability conditions for a simplified ESC model have been summarized in [41]: "If the average model of ESC is asymptotically stable, $1/\omega$ is sufficiently small and the initial conditions are small in an appropriate sense, then the theorem would claim the existence of an exponentially stable periodic solution which is at a distance that continuously depends on $1/\omega$, a, and k ".

1) Averaged Linearized Model for Simplified ESC Algorithm: Averaged linearized model for the simplified IO-ESC feedback loop, shown in Fig. 3, relating the optimized point, θ^*, and the error signal, $\tilde{\theta} = \theta - \theta^*$, has been derived as [41]

$$\frac{\tilde{\theta}}{\theta^*} = \frac{1}{1+L(s)}, \tag{5}$$

where

$$L(s) = \frac{ka^2}{2s}\left(e^{j\phi}\frac{s+j\omega}{s+j\omega+\omega_h} + e^{-j\phi}\frac{s-j\omega}{s-j\omega+\omega_h}\right). \tag{6}$$

ϕ is the phase delay of the perturbation signal. If $\phi = 0$, then (5) becomes

$$\frac{\tilde{\theta}(s)}{\theta^*(s)} = \frac{s(s^2+2\omega_h s+\omega_h^2+\omega^2)}{s^3+(2\omega_h+ka^2)s^2+(\omega_h^2+\omega^2+ka^2\omega_h)s+ka^2\omega^2}. \tag{7}$$

By looking at (7), one can conclude that $\frac{\tilde{\theta}}{\theta^*}$ is asymptotically stable for all $k > 0$.

The averaged linearized model is one of the approaches to check the stability of any nonlinear system [42]. Thus (5) can be employed specifically to test the stability of ESC loop as mentioned in [38] and [41].

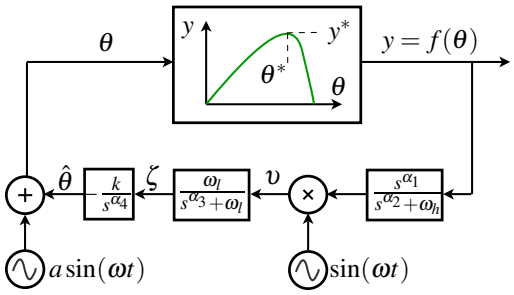

Fig. 4. Fractional Order Extremum Seeking Control Scheme

In the following sections, FO-ESC is introduced and by employing averaged linearized model, the advantages of using fractional order operators in the ESC structure, from the stability and transient response point of view are investigated.

IV. Fractional Order Extremum Seeking Control

As mentioned before, ESC is an online adaptive optimization algorithm which drives the process to its optimal operating point where the defined cost function is minimized or maximized. This controller consists of three main components:

- The performance (objective) function which includes unknown parameters,
- The gradient estimator to approximate the variation direction, and
- The optimizer which maximize (minimize) the objective function.

By employing fractional order filters in the gradient estimator and optimizer of ESC, fractional order extremum seeking control will be born. The general block diagram of FO-ESC is depicted in Fig. 4 and its mathematical model can be written as

$$\begin{cases} y = f(\hat{\theta} + a\sin(\omega t)) \\ D^{\alpha_4}\hat{\theta} = -k\zeta \\ \zeta = \upsilon * \mathscr{L}^{-1}\{\frac{\omega_l}{s^{\alpha_3}+\omega_l}\} \\ \upsilon = \left(y * \mathscr{L}^{-1}\{\frac{s^{\alpha_1}}{s^{\alpha_2}+\omega_h}\}\right)\sin(\omega t) \end{cases}, \tag{8}$$

where D^{α} is the Riemann-Liouville fractional order derivative and $\alpha_i \in \mathbb{R}, i = 1,2,3,4$.

For the same reasons which were discussed in the previous section, fractional order low-pass filter can be eliminated in this structure. Moreover, stability study for general form of fractional order LTI system is not trivial and for one to be able to analyze the stability of FO-ESC, this system should be in the form of irrational order system which implies $\alpha_i (i = 1,2,3,4) = q$ and $q \in \mathbb{R}$ [29]. Considering these points, FO-ESC of Fig. 4, can be reduced to the depicted structure in Fig. 5 and its mathematical model will be

$$\begin{cases} y = f(\hat{\theta} + a\sin(\omega t)) \\ D^{q}\hat{\theta} = -k\upsilon \\ \upsilon = \left(y * \mathscr{L}^{-1}\{\frac{s^q}{s^q+\omega_h}\}\right)\sin(\omega t) \end{cases}. \tag{9}$$

In order to check the stability of FO-ESC, the generalized averaged linearized model between optimal point, θ^*, and

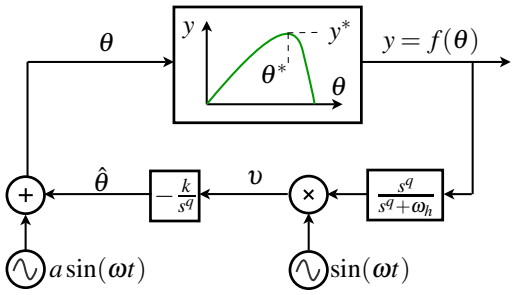

Fig. 5. Simplified Fractional Order Extremum Seeking Control Scheme

error signal, $\tilde{\theta}$, for FO-ESC should be derived. As mentioned before, this model can be a valid indicator to justify and check the stability of ESC feedback loop. To obtain this averaged model, "Modulation property" lemma for fractional order systems needs to be proved. This lemma is the generalized form of the lemmas in [41] which has been demonstrated for the specific case of integer order systems. For one to compare this proof with [41], authors use the same notations.

Note 1: $H(s)[u(t)]$ means a system with transfer function $H(s)$ driven by a time domain signal, $u(t)$ or mathematically speaking $H(s)[u(t)] = \mathscr{L}^{-1}\{H(s)\} * u(t)$. The output of this notation is a signal in time domain.

Note 2: $H(s^q)$ is the notation for any LTI commensurate order system which means

$$H(s^q) = \frac{\sum_{k=0}^{M} b_k (s^q)^k}{\sum_{k=0}^{N} a_k (s^q)^k} = \frac{Z(s^q)}{P(s^q)}. \tag{10}$$

Lemma 1: (Modulation property for fractional order systems) If all poles of a commensurate order system, $H(s^q) = \frac{Z(s^q)}{P(s^q)}$, are stable (means $\arg(\lambda_i^q) > \frac{\pi q}{2}$ and λ_is are roots of $P(s^q)$), then for any real φ,

$$H(s^q)[\sin(\omega t - \varphi)] = Im\{H\big((j\omega)^q\big)e^{j(\omega t-\varphi)}\} + \varepsilon^{-t}. \tag{11}$$

Proof:

$$\begin{aligned}
&H(s^q)[\sin(\omega t - \varphi)] = H(s^q)[Im\{e^{j(\omega t-\varphi)}\}] \\
&= \frac{1}{2j} H(s^q)[e^{-j(\omega t-\varphi)} - e^{j(\omega t-\varphi)}] \\
&= \frac{1}{2j}\mathscr{L}^{-1}\{H(s^q)\frac{1}{s-j\omega}e^{-j\varphi} - H(s^q)\frac{1}{s+j\omega}e^{j\varphi}\} \\
&= \frac{1}{2j}\mathscr{L}^{-1}\Big\{\underbrace{\frac{Z(s^q)(j\omega+s)e^{-j\varphi} + (j\omega-s)e^{j\varphi}}{P(s^q)(s^2+\omega^2)}}_{Y(s,s^q)}\Big\}.
\end{aligned} \tag{12}$$

By applying partial fraction decomposition to $Y(s,s^q)$, as described in [29] and [32], the residuals for each pole of $Y(s,s^q)$ are

$$Q_i(s^q)_{i=1,\ldots,N} = \Lambda_i(s^q)Y(s,s^q)\mid_{s,s^q=\lambda_i}, \tag{13}$$

where λ_i's are the poles of $Y(s,s^q)$ and $\Lambda_i(s^q)$'s are the factors of $P(s^q)$ such that $P(s^q) = \prod_{i=1}^{N}\Lambda_i$.

Residuals for two known poles of $Y(s,s^q)$ at $\lambda_{1,2} = \pm j\omega$ are $\frac{H((j\omega)^q)}{s-j\omega}e^{-j\varphi}$ and $\frac{-H(-(j\omega)^q)}{s+j\omega}e^{j\varphi}$. Therefore (12) becomes

$$\begin{aligned}
&= \frac{1}{2j}\mathscr{L}^{-1}\Big\{H((j\omega)^q)\frac{1}{s-j\omega}e^{-j\varphi} - H(-(j\omega)^q)\frac{1}{s+j\omega}e^{j\varphi} \\
&+ \underbrace{\sum_{i=3}^{N}\frac{Q_i(s^q)}{\Lambda_i(s^q)}}_{\varepsilon^{-t}}\Big\}.
\end{aligned} \tag{14}$$

Without lose of generality, λ_i are assumed to be simple poles. Since all poles of $H(s^q)$ are stable poles, $\sum_{i=3}^{N}\frac{Q_i(s^q)}{\Lambda_i(s^q)}$ decays exponentially and these terms does not affect the steady state response of the system. Therefore,

$$\begin{aligned}
&H(s^q)[\sin(\omega t - \varphi)] \\
&= \frac{1}{2j}\mathscr{L}^{-1}\Big\{\frac{H((j\omega)^q)}{s-j\omega}e^{-j\varphi} - \frac{H(-(j\omega)^q)}{s+j\omega}e^{j\varphi}\Big\} + \varepsilon^{-t} \\
&= Im\{H\big((j\omega)^q\big)e^{j(\omega t-\varphi)}\} + \varepsilon^{-t}.\diamond
\end{aligned} \tag{15}$$

ε^{-t} denotes an exponential decaying function.

Lemma 2: If fractional order systems, $G(s^\beta)$ and $H(s^\alpha)$, are stable, then for any real φ and a uniformly bounded $u(t)$,

$$\begin{aligned}
&G(s^\beta)[(H(s^\alpha)[\sin(\omega t - \varphi)])u(t)] \\
&= Im\Big\{H((j\omega)^\alpha)e^{j(\omega t-\varphi)} \\
&H((j\omega)^\alpha)G(s^\beta + j\omega)[u(t)]\Big\} + \varepsilon^{-t}.
\end{aligned} \tag{16}$$

Proof: From Lemma 1,

$$\begin{aligned}
&G(s^\beta)[H(s^\alpha)[\sin(\omega t - \varphi)]u(t)] \\
&= G(s^\beta)[Im\{H((j\omega)^\alpha)e^{j(\omega t-\varphi)}\}[u(t) + \varepsilon^{-t}] \\
&= Im\{e^{-j\varphi}\mathscr{L}^{-1}\{G(s^\beta)H((j\omega)^\alpha)U(s-j\omega)\}\} + \varepsilon^{-t}.
\end{aligned} \tag{17}$$

If $G(s^\beta) \xrightarrow{\mathscr{L}^{-1}} g(t)$ and $U(s) \xrightarrow{\mathscr{L}^{-1}} u(t)$, then,

$$\begin{aligned}
&\mathscr{L}^{-1}\{G(s^\beta)U(s-j\omega)\} = g(t) \star u(t)e^{j\omega t} \\
&= \int_{-\infty}^{+\infty} g(\tau)u(t-\tau)e^{j\omega(t-tau)}d\tau \\
&= e^{j\omega t}\int_{-\infty}^{+\infty} g(\tau)e^{-j\omega\tau}u(t-\tau)d\tau \\
&= e^{j\omega t}\mathscr{L}^{-1}\{G(s^\beta + j\omega)U(s)\}.
\end{aligned} \tag{18}$$

Therefore, (17) can be rewritten as

$$\begin{aligned}
&Im\{e^{-j\varphi}\mathscr{L}^{-1}\{G(s^\beta)H((j\omega)^\alpha)U(s-j\omega)\}\} + \varepsilon^{-t} \\
&= Im\Big\{e^{j(\omega t-\varphi)}H((j\omega)^\alpha)\mathscr{L}^{-1}\{G(s^\beta + j\omega)U(s)\}\Big\} + \varepsilon^{-t} \\
&= Im\Big\{e^{j(\omega t-\varphi)}H((j\omega)^\alpha)G(s^\beta + j\omega)[u(t)]\Big\} + \varepsilon^{-t}.\diamond
\end{aligned} \tag{19}$$

Using Lemma 1 and Lemma 2, it can be easily verified that for fractional order systems, $A(.)$ and $B(.,.)$, the following is true:

$$
\begin{aligned}
&Im\{e^{j(\omega t-\varphi)}A(s^q)\}Im\{e^{j(\omega\tau-\phi)}B(s^q,(j\omega)^q))[z(t)]\}\\
&=\frac{1}{2}Re\{e^{j(\varphi-\phi)}A((-j\omega)^q)B(s^q,(j\omega)^q)[z(t)]\}\\
&-\frac{1}{2}Re\{e^{j(2\omega\tau-\varphi-\phi)}A((-j\omega)^q)B(s^q,(j\omega)^q)[z(t)]\}. \qquad (20)
\end{aligned}
$$

A. Stability Analysis of FO-ESC

By substituting $\hat{\theta}$ with its equivalent term $\theta - a\sin(\omega t)$ and applying Laplace transform, the mathematical model for FO-ESC, (9), can be rewritten as,

$$
\begin{cases}
y = f(\theta)\\
\theta = a\sin(\omega t) - \frac{k}{s^q}[\upsilon]\\
\upsilon = \sin(\omega t)\frac{s^q}{s^q+\omega_h}[y]
\end{cases}. \qquad (21)
$$

To linearize the nonlinear plant around its optimal point, θ^*, Taylor expansion is employed.

$$
y = f(\theta^*) + \dot{f}(\theta^*)(\theta-\theta^*) + \frac{1}{2}\ddot{f}(\theta^*)(\theta-\theta^*)^2 + HOT, \qquad (22)
$$

where HOT stands for higher order terms. Since θ^* is an extremum point $\dot{f}(\theta^*)=0$ also $\ddot{f}(\theta^*)$ can be absorbed in integrator gain of ESC algorithm [41], therefore combining (22) and (21) and applying above considerations, one can obtain

$$
\begin{cases}
y = f^* + (\theta^*-\theta)^2\\
\theta = a\sin(\omega t) - \frac{k}{s^q}[\upsilon]\\
\upsilon = \sin(\omega t)\frac{s^q}{s^q+\omega_h}[y]
\end{cases}, \qquad (23)
$$

where $f^* = f(\theta^*)$.

By defining $\tilde{\theta} = \theta^* - \theta + a\sin(\omega t)$ and substituting and combining equations form (23) into this definition, one gets

$$
\begin{aligned}
\tilde{\theta} &= \theta^* + \frac{k}{s^q}\Big[\sin(\omega t)\frac{s^q}{s^q+\omega_h}[y]\Big]\\
&= \theta^* + \frac{k}{s^q}\Big[\sin(\omega t)\frac{s^q}{s^q+\omega_h}[f^* + (\underbrace{\theta-\theta^*}_{\tilde{\theta}-a\sin(\omega t)})^2]\Big]\\
&= \theta^* + \frac{k}{s^q}\Big[\sin(\omega t)\frac{s^q}{s^q+\omega_h}[f^*] + \sin(\omega t)\frac{s^q}{s^q+\omega_h}[\tilde{\theta}^2]\\
&+ \sin(\omega t)\frac{s^q}{s^q+\omega_h}[a^2\sin^2(\omega t)]\\
&- 2a\sin(\omega t)\frac{s^q}{s^q+\omega_h}[\tilde{\theta}][\sin(\omega t)]\Big]. \qquad (24)
\end{aligned}
$$

Replacing $sin(\omega t)$ with its equivalent term $Im\{e^{j\omega t}\}$, and applying Lemma 2 to the last term of (24) (define $G(s^q) = \frac{s^q}{s^q+\omega_h}$) and eliminating the exponentially decaying terms (ε^{-t}) gives

$$
\begin{aligned}
&2a\sin(\omega t)\frac{s^q}{s^q+\omega_h}[\tilde{\theta}][\sin(\omega t)]\\
&= 2aIm\{e^{j\omega t}\}Im\{e^{j\omega t}\frac{s^q+j\omega}{s^q+\omega_h+j\omega}\}[\tilde{\theta}]\\
&= aRe\{\frac{s^q+j\omega}{s^q+\omega_h+j\omega}\}[\tilde{\theta}]\} - aRe\{e^{2j\omega t}\frac{s^q+j\omega}{s^q+\omega_h+j\omega}\}[\tilde{\theta}]\}. \qquad (25)
\end{aligned}
$$

Replacing the last term of (24) with its equivalent, (25), and moving LTI parts of the result to the left side of the equation and time varying terms to the right side, (24) becomes

$$
\begin{aligned}
&\tilde{\theta} + \frac{ak}{s^q}Re\{\frac{s^q+j\omega}{s^q+\omega_h+j\omega}\}[\tilde{\theta}]\} \qquad (26)\\
&= \theta^* + \frac{k}{s^q}\Big[\sin(\omega t)\frac{s^q}{s^q+\omega_h}[f^*] + \sin(\omega t)\frac{s^q}{s^q+\omega_h}[\tilde{\theta}^2]\\
&+ \sin(\omega t)\frac{s^q}{s^q+\omega_h}[a^2\sin^2(\omega t)]\\
&- aRe\{e^{2j\omega t}\frac{s^q+j\omega}{s^q+\omega_h+j\omega}\}[\tilde{\theta}]\}\Big]. \qquad (27)
\end{aligned}
$$

By substituting $s^q = \eta$ and applying periodic averaging theorem, as described in [41], the averaged linearized model relating the optimized point, θ^*, and the error signal, $\tilde{\theta}$, in the generalized simplified ESC is derived as,

$$
\frac{\tilde{\theta}}{\theta^*} = \frac{1}{1+L(s)}, \qquad (28)
$$

where $L(s)$ will be

$$
\frac{\tilde{\theta}(\eta)}{\theta^*(\eta)} = \frac{\eta(\eta^2+2\omega_h\eta+\omega_h^2+\omega^2)}{\eta^3+(2\omega_h+ka^2)\eta^2+(\omega_h^2+\omega^2+ka^2\omega_h)\eta+ka^2\omega^2}. \qquad (29)
$$

This relationship is the generalized averaged linearized model between the optimized point, θ^*, and the error signal, $\tilde{\theta}$. As can be seen from (29), in the case of IO-ESC, by changing η to s, the linearized averaged model of (7), which has been derived in [41], is confirmed.

In the case of FO-ESC, this model is

$$
\frac{\tilde{\theta}(s^q)}{\theta^*(s^q)} = \frac{s^q(s^{2q}+2\omega_h s^q+\omega_h^2+\omega^2)}{s^{3q}+(2\omega_h+ka^2)s^{2q}+(\omega_h^2+\omega^2+ka^2\omega_h)s^q+ka^2\omega^2}. \qquad (30)
$$

In the following section, FO-ESC and IO-ESC will be compared using derived averaged linearized models.

V. Stability Analysis of Simplified ESC Algorithms

Before investigating the stability analysis of proposed ESC algorithm, it should be noted that the stability region for LTI fractional order systems is different from LTI integer order systems. It is well-known that an integer order LTI system is stable if all the roots of the characteristic polynomial are located on the left side of the imaginary axis of the complex s-plane. By mapping the stable region of LTI integer order systems under s^q transformation, the stable region from s-plane transforms to sector $|\varphi| > q\pi/2$. Thus, the LTI fractional order systems is stable if all roots in the s-plane lies in the region $|\varphi| > q\pi/2$ [43]. This region depicted in Fig. 6.

As discussed before, the linearized averaged model can be used to analyze the stability of ESC. The general linearized averaged model for a simplified IO-ESC algorithm shown in (7) has three poles at $\lambda_i = a_k \pm jb_k = r_k\angle\varphi_k$, where $k = 1,2,3$. and r_k and φ_k are the amplitude and phase of the integer order poles respectively.

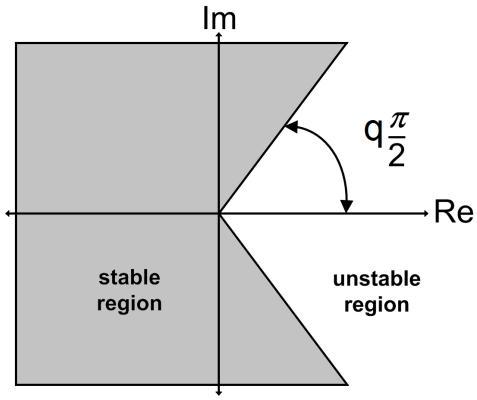

Fig. 6. Stability Region for Fractional Order Systems

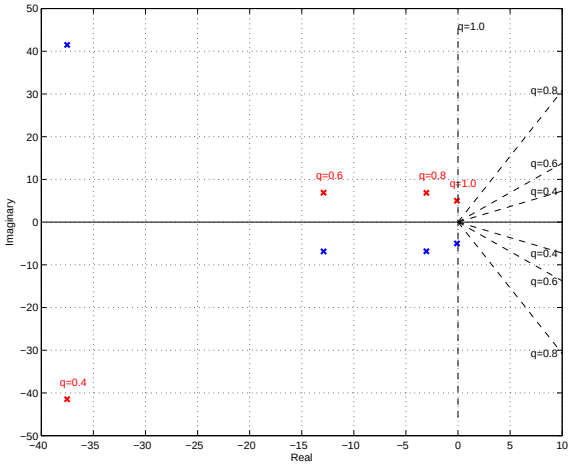

Fig. 7. Poles of IO-ESC and FO-ESC Averaged Linear Models

On the other hand, The general linearized averaged model poles for a simplified FO-ESC algorithm shown in (30) are mapped to $\lambda_f = r_k^{(1/q)} \angle(\varphi/q) = r_{f_k} \angle \varphi_{f_k}$, where r_{f_k} and φ_{f_k} are the amplitude and phase of the fractional order poles respectively. Knowing $0 < q < 1$, $|Re\{\lambda_f\}| = r_{f_k}$ will be greater than $|Re\{\lambda_i\}| = r_k$ as long as $\varphi_f \in [-\pi/2, \pi/2]$

As an example, Fig. 7 illustrates the relative locations of mapped fractional order poles with different orders ($q = 0.4, 0.6, 0.8$) while the initial integer order poles are located at $0.1 \pm 5j$. Moreover, the stability boundaries for different q's are depicted. Since, the farther the eigenvalues from the instability boundaries, the more stable the system is, consequently, fractional order eigenvalues will have monotonically decreasing response unlike the integer order ones which will have lightly damped response. This feature helps the FO-ESC to have better settling time.

Considering distance of the eigenvalues from instabilities boundaries, it can be claimed that integer order system with eigenvalues close to imaginary axis may become unstable with even a small disturbance, uncertainty or noise. This point demonstrates the advantage of FO-ESC over the IO-ESC from the aspect of robustness. In other words, FO-ESC will be more robust against system uncertainty because its eigenvalues can tolerate more amount of deviations before they enter to their unstable region.

A. Simulation and Experimental Results

In order to compare the performance of IO-ESC and FO-ESC, a horsepower dynamometer, shown in Fig. 8, is employed.

Generally, dynamometer or "Dyno" is a device for measuring force, torque, or power of an engine, motor or other rotating prime mover. This dynamometer includes a DC motor which is mechanically coupled to a hysteresis brake used to apply load to the motor. A load cell measures the amount of load which is applied to the motor shaft and an optical encoder and a tachometer provides the position and angular velocity of the shaft respectively.

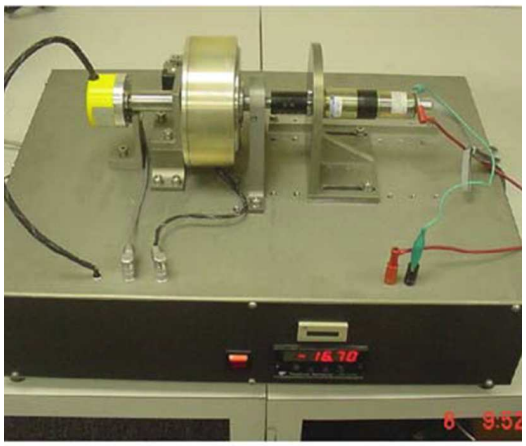

Fig. 8. Horsepower Dynamometer

According to its structure, Dyno can be modeled as a servo system which can be presented as,

$$\begin{aligned} \dot{x}(t) &= Kv(t) \\ \dot{v}(t) &= -\frac{1}{\tau}v(t) + u(t) + f(t,x) \end{aligned} \tag{31}$$

where $v(t)$ is the shaft speed, $u(t)$ is the input voltage, $x(t)$ is the shaft displacement, K is the system gain, τ is the time constant of the system and $f(t,x)$ is the load disturbance caused by hysteresis brake. Having $f(t,x)$ in the equation give the ability to add a time-dependent or state-dependent disturbances to the motor. Servo system dynamic equation is widely used to model various mechanical structures, e.g. active suspension system [44], [45] , [46], electromechanical throttle [47], etc.

Gain and time constant for the benchmarked dynamometer are $K = 1.52$, $\tau = 1.01s$ [48] and $f(t,x)$ is assumed to be a nonlinear function with one extremum point as shown in Fig. 9

This article has been accepted for publication in a future issue of this journal, but has not been fully edited. Content may change prior to final publication. Citation information: DOI 10.1109/TMECH.2016.2517621, IEEE/ASME Transactions on Mechatronics

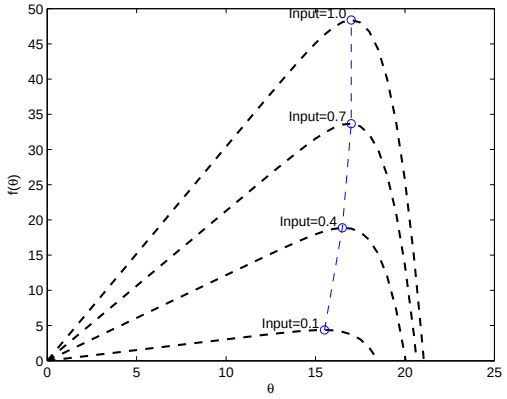

Fig. 9. Static Nonlinear System Responses for Different Inputs

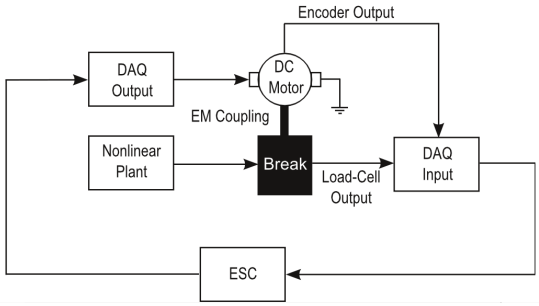

Fig. 10. Schematic of Applying Nonlinear Disturbance to the Horsepower Dynamometer

As can be seen in this figure, the output (and extremum point) of this nonlinear function mainly depends on the input terminal and thus extremum seeking control can be a viable option to extract maximum point. The architecture of the dynamometer system used for this work is shown in Fig. 10.

To compare the performance of IO-ESC and FO-ESC numerically, these two algorithms are applied to the MATLAB/Simulink model of Fig. 10 To make a fair comparison, both algorithms run under the same conditions and use the same tuning values. In this simulation, gain of ESC integrator is set to be $k = 15$, perturbation frequency and amplitude are $\omega = 100 rad/s$ and $a = 0.1$ respectively, cut-off frequency for high-pass filter is $\omega_h = 50 rad/s$ and order of FO-ESC is set to be $q = 0.9$. This order applies both to the integrator and high-pass filter. Moreover, CRONE toolbox is used to implement the fractional order operators.

Figure 11 shows the convergence speed of IO-ESC and FO-ESC and as can be seen in this figure, FO-ESC can stick to the extremum point almost two times faster than IO-ESC.

Figure 12 shows the experimental responses of IO-ESC and FO-ESC. Although the numerical and experimental responses are not identical which is the results of un-modeled dynamics of the system, but as can be seen, FO-ESC reaches to extremum point almost two times faster than IO-ESC which admits the results achieved from the numerical simulation and mathematical analysis.

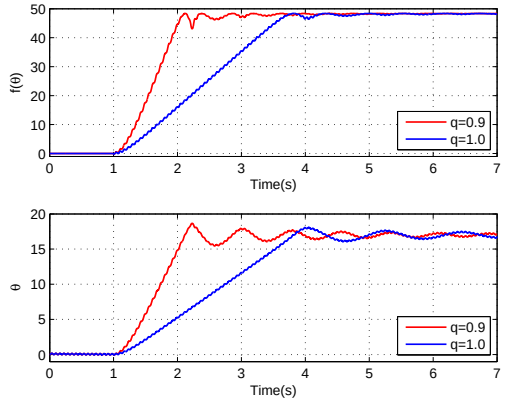

Fig. 11. Simulation Results of Performance Comparison Between IO-ESC and FO-ESC

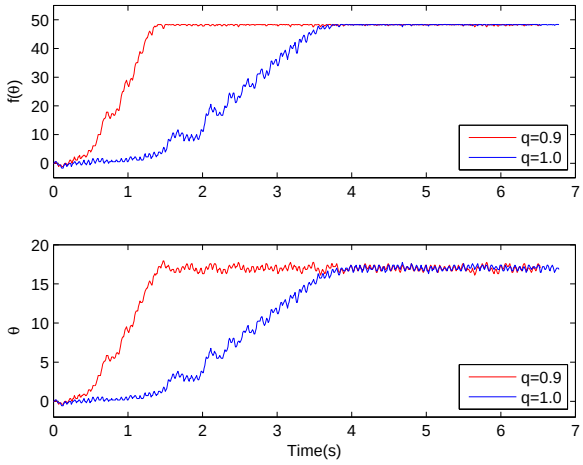

Fig. 12. Experimental Results of Performance Comparison Between IO-ESC and FO-ESC

VI. Conclusion

In this paper, a novel extremum seeking control algorithm which utilizes the fractional order operators was introduced, analyzed and compared against integer order extremum seeking control. Unlike other proposed ESC algorithms, FO-ESC does not employ additional feedback loops or switching methods to improve the performance of the algorithm. Mathematical analysis on this algorithm was performed using linearized averaging model. These analysis show how special features of fractional order operators affect and improve the overall convergence and robustness properties of the extremum seeking algorithm. Numerical evaluations using MATLAB/Simulink and experimental results using dynamometer, provide a solid justification for the remarkable performance enhancement in the face of uncertainties and noise.

References

[1] X. Li, Y. Li, and J. Seem, "Maximum power point tracking for photovoltaic system using adaptive extremum seeking control," *IEEE Transactions on Control Systems Technology*, vol. 21, no. 6, pp. 2315–2322, Nov 2013.

[2] R. Leyva, C. Olalla, H. Zazo, C. Cabal, A. Cid-Pastor, I. Queinnec, and C. Alonso, "MPPT based on sinusoidal extremum-seeking control in PV generation," *International Journal of Photoenergy*, vol. 98, no. 4, pp. 529–542, Apr. 2011.

[3] S. J. Moura and Y. A. Chang, "Lyapunov-based switched extremum seeking for photovoltaic power maximization," *Control Engineering Practice*, vol. 21, no. 7, pp. 971–980, 2013.

[4] J.-H. Chen, H.-T. Yau, and W. Hung, "Design and study on sliding mode extremum seeking control of the chaos embedded particle swarm optimization maximum power point tracking in wind power system," *energies*, vol. 7, pp. 1706–1720, 2014.

[5] T. Pan, Z. Ji, and Z. Jiang, "Maximum power point tracking of wind energy conversion systems based on sliding mode extremum seeking control," in *IEEE Energy 2030 Conference*, Nov 2008, pp. 1–5.

[6] A. Ghaffari, M. Krstic, and S. Seshagiri, "Power optimization for photovoltaic microconverters using multivariable newton-based extremum seeking," *IEEE Transactions on Control Systems Technology*, vol. 22, no. 6, pp. 2141–2149, Nov. 2014.

[7] E. Dincmen, B. Guvenc, and T. Acarman, "Extremum-seeking control of ABS braking in road vehicles with lateral force improvement," *IEEE Transactions on Control Systems Technology*, vol. 22, no. 1, pp. 230–237, Jan 2014.

[8] C. Zhang and R. Ordez, *Extremum-Seeking Control and Applications: A Numerical Optimization-Based Approach*. Springer, 2012.

[9] S. Drakunov, U. Ozguner, P. Dix, and B. Ashra, "A ABS control using optimum search via sliding modes," *IEEE Transactions on Control Systems Technology*, vol. 3, pp. 79–85, 1995.

[10] N. J. Killingsworth, S. M. Aceves, D. L. Flowers, F. Espinosa-Loza, and M. Krstic, "HCCI engine combustion-timing control: Optimizing gains and fuel consumption via extremum seeking," *IEEE Transactions on Control Systems Technology*, vol. 17, no. 6, pp. 1350–1361, 2009.

[11] E. Hellstrom, D. Lee, L. Jiang, A. Stefanopoulou, and H. Yilmaz, "On-board calibration of spark timing by extremum seeking for flex-fuel engines," *IEEE Transactions on Control Systems Technology*, vol. 21, no. 6, pp. 2273–2279, Nov. 2013.

[12] Y. Zhang and N. Gans, "Extremum seeking control of a nonholonomic mobile robot with limited field of view," in *American Control Conference (ACC13)*, June 2013, pp. 2765–2771.

[13] Y. Tian and N. Sarkar, "Control of a mobile robot subject to wheel slip," *Journal of Intelligent & Robotic Systems*, vol. 74, no. 3-4, pp. 915–929, 2014.

[14] N. Ghods, "Extremum seeking for mobile robots," Ph.D. dissertation, University of California, San Diego, 2011.

[15] P. Binetti, K. Ariyur, M. Krstic, and F. Bernelli, "Control of formation flight via extremum seeking," in *Proceedings of the American Control Conference (ACC02)*, vol. 4, 2002, pp. 2848–2853 vol.4.

[16] D. Dochain, M. Perrier, and M. Guay, "Extremum seeking control and its application to process and reaction systems: A survey," *Mathematics and Computers in Simulation*, vol. 82, no. 3, pp. 369–380, 2011.

[17] Y. Tan, W. Moase, C. Manzie, D. Nesic, and I. M. Y. Mareels, "Extremum seeking from 1922 to 2010," in *29th Chinese Control Conference (CCC10)*, July 2010, pp. 14–26.

[18] D. Nesic, "Extremum seeking control: Convergence analysis," *European Journal of Control*, vol. 15, no. 3-4, pp. 331–347, 2009.

[19] Y. Tan, D. Nesic, and I. Mareels, "On the choice of dither in extremum seeking systems: A case study," *Automatica*, vol. 44, no. 5, pp. 1446 – 1450, 2008.

[20] Y. Pan, m. zgner, and T. Acarman, "Stability and performance improvement of extremum seeking control with sliding mode," *International Journal of Control*, vol. 76, no. 9-10, pp. 968–985, 2003.

[21] B. Calli, W. Caarls, P. Jonker, and M. Wisse, "Comparison of extremum seeking control algorithms for robotic applications," in *Intelligent Robots and Systems (IROS), 2012 IEEE/RSJ International Conference on*, Oct 2012, pp. 3195–3202.

[22] Y.-a. Hu, B. Zuo, and J. Li, "A novel chaotic annealing recurrent neural network for multi-parameters extremum seeking algorithm," in *Neural Information Processing*, ser. Lecture Notes in Computer Science, I. King, J. Wang, L.-W. Chan, and D. Wang, Eds. Springer Berlin Heidelberg, 2006, vol. 4233, pp. 1022–1031.

[23] S. Moura and Y. Chang, "Asymptotic convergence through lyapunov-based switching in extremum seeking with application to photovoltaic systems," in *American Control Conference (ACC)*, June 2010, pp. 3542–3548.

[24] C. Yin, Y. Chen, and S. ming Zhong, "Fractional-order sliding mode based extremum seeking control of a class of nonlinear systems," *Automatica*, vol. 50, no. 12, pp. 3173 – 3181, 2014.

[25] C. Li, Z. Qu, and M. A. Weitnauer, "Distributed extremum seeking and formation control for nonholonomic mobile network," *Systems & Control Letters*, vol. 75, pp. 27–34, 2015.

[26] R. Singh, M. P. Kearney, and C. Manzie, "Improving performance of extremum-seeking control applied to a supercritical-CO2 closed brayton cycle in a solar thermal power plant," in *The 4th International Symposium Supercritical CO2 Power Cycles*, Pittsburgh, Pennsylvania, Sept. 2014.

[27] A. Ghaffari, M. Krstic, and D. Nesic, "Multivariable newton-based extremum seeking," *Automatica*, vol. 48, no. 8, pp. 1759 – 1767, 2012.

[28] C. Olalla, M. I. Arteaga, R. Leyva, and A. El Aroudi, "Analysis and comparison of extremum seeking control techniques," in *IEEE International Symposium on Industrial Electronics (ISIE07)*, 2007, pp. 72–76.

[29] C. A. Monje, Y. Chen, B. M. Vinagre, D. Xue, and V. Feliu-Batlle, *Fractional-order Systems and Controls: Fundamentals and Applications (Advances in Industrial Control)*. New York: Springer, 2010.

[30] I. Podlubny, *Fractional Differential Equations. An Introduction to Fractional Derivatives, Fractional Differential Equations, Some Methods of Their Solution and Some of Their Applications*. San Diego: Academic Press, 1999.

[31] Y. Chen, "Ubiquitous Fractional order Controls?" in *Proceedings of 2nd IFAC Symposium on Fractional Derivatives and Applications (IFAC FDA06)*, Porto, Portugal, 2006.

[32] I. Petras, *Fractional Order Nonlinear Systems, Modeling, Analysis and Simulation*. New York: Springer, 2011.

[33] H. Malek, Y. Luo, and Y. Chen, "Identification and tuning fractional order proportional integral controllers for time delayed systems with a fractional pole," *Mechatronics*, vol. 23, no. 7, pp. 746–754, Oct. 2013.

[34] Y. Chen and K. L. Moore, "Discretization schemes for fractional-order differentiators and integrators," *IEEE Transactions on Circuit and Systems*, vol. 49, no. 3, pp. 363–367, Mar. 2002.

[35] M. Romero, B. M. Vinagre, and A. P. de Madrid, "GPC control of a fractional-order plant: Improving stability and robustness," in *Proceedings of the 17th IFAC World Congress*, vol. 17, no. 1, South Korea, July 2008, pp. 14 266–14 271.

[36] M. Pakzad, S. Pakzad, and M. Nekoui, "Stability analysis of multiple time delayed fractional order systems," in *American Control Conference (ACC), 2013*, June 2013, pp. 170–175.

[37] I. Petras, "Stability of fractional order systems with rational order: A survey," *Fractional Calculus and Applied Analysis*, vol. 12, no. 3, pp. 269–298, 2009.

[38] M. Krstic and H. Wang, "Stability of extremum seeking feedback for general nonlinear dynamic systems," *Automatica*, vol. 36, pp. 595–601, 2000.

[39] J. Dandois and P.-Y. Pamart, "NARX modeling and extremum-seeking control of a separation," *Journal of Aerospace Lab*, vol. 6, June 2013.

[40] K. B. Ariyur and M. Krstic, *Real-Time Optimization by Extremum-Seeking Control*. Hoboken: Wiley-Interscience, 2003.

[41] M. Krstic, "Performance improvement and limitations in extremum seeking control," *Systems and Control Letters*, vol. 39, no. 5, pp. 313–326, 2000.

[42] H. Khalil, *Nonlinear Systems*. Englewood Cliffs, NJ: Prentice-Hall, 1996.

[43] I. Petras and S. Grega, "Digital fractional order controllers realized by PIC microprocessor: Experimental results," in *Proceedings of the International Carpathian Control Conference (ICCC03)*, High Tatras, Slovak Republic, May 2003, pp. 873–876.

[44] W. Sun, H. Gao, and O. Kaynak, "Finite frequency h control for vehicle active suspension systems," *IEEE Transactions on Control Systems Technology*, vol. 19, no. 2, pp. 416–422, March 2011.

[45] H. Pan, W. Sun, H. Gao, and J. Yu, "Finite-time stabilization for vehicle active suspension systems with hard constraints," *IEEE Transactions on Intelligent Transportation Systems*, vol. 16, no. 5, pp. 2663–2672, Oct 2015.

[46] W. Sun, H. Gao, and O. Kaynak, "Vibration isolation for active suspensions with performance constraints and actuator saturation," *IEEE/ASME Transactions on Mechatronics*, vol. 20, no. 2, pp. 675–683, April 2015.

[47] R. Grepl and B. Lee, "Modeling, parameter estimation and nonlinear control of automotive electronic throttle using a rapid-control prototyping technique," *International Journal of Automotive Technology*, vol. 11, no. 4, pp. 601–610, 2010.

[48] Y. Tarte, Y.-Q. Chen, W. Ren, and K. Moore, "Fractional horsepower dynamometer - A general purpose hardware-in-the-loop real-time simulation platform for nonlinear control research and education," in *Proceedings of 45th IEEE Conference on Decision and Control (CDC06)*, Dec. 2006, pp. 3912–3917.